Mat. Res. Soc. Symp. Proc. Vol. 674 © 2001 Materials Research Society

The Role of Disorder in the Magnetic Properties of Mechanically Milled Nanostructured Alloys

Diandra L. Leslie-Pelecky[1], Elaine M. Kirkpatrick[1], Tom Pekarek[2], Richard L. Schalek[3], Paul Shand[4], Deborah S. Williams[1], and Lanping Yue[1]

[1]Center for Materials Research and Analysis and Department of Physics & Astronomy, University of Nebraska, Lincoln NE 68588-0111
[2]Department of Chemistry and Physics, University of North Florida, Jacksonville, FL 32224
[3]Composite Materials and Structures Center, Michigan State University, East Lansing MI, 48824
[4]Physics Department, University of Northern Iowa, Cedar Falls, Iowa 50614

ABSTRACT

Mechanical milling provides a unique means of studying the influence of grain size and disorder on the magnetic properties of nanostructured alloys. This paper compares the role of milling in the nanostructure evolution of two ferromagnets – $SmCo_5$ and $GdAl_2$ – and the subsequent impact of nanostructure on magnetic properties and phase transitions. The ferromagnetic properties of $SmCo_5$ are enhanced by short (< 2 hours) milling times, producing up to an eight-fold increase in coercivity and high remanence ratios. The coercivity increase is attributed to defect formation and strain. Additional milling increases the disorder and produces a mix of ferromagnetic and antiferromagnetic interactions that form a magnetically glassy phase. $GdAl_2$, which changes from ferromagnetic in its crystalline form to spin-glass-like in its amorphous form, is a model system for studying the dependence of magnetically glassy behavior on grain size and disorder. Nanostructured $GdAl_2$ with a mean grain size of 8 nm shows a combination of ferromagnetic and magnetically glassy behavior, in contrast to previous studies of nanostructured $GdAl_2$ with a grain size of 20 nm that show only spin-glass-like behavior.

INTRODUCTION

Mechanical milling is a high-energy deformation process that progressively introduces defect structures (dislocations and vacancies), atomic-scale chemical disorder and elastic strain energy into the initially crystalline starting powders through the shearing actions of ball-powder collisions [1,2]. Mechanical milling can be used to produce a variety of effects in intermetallic alloys due to the complex dependence of the nanostructure on milling intensity, temperature, and other factors [3]. The magnetic properties of a nanostructure depend on the intrinsic material properties, but also on grain size and grain size distribution, the magnetic character of the interphase (the region between grains), and the intergrain magnetic coupling. The challenge is to separate the different contributions to the overall magnetic properties by carefully controlling and characterizing nanostructure. The versatility of mechanical milling makes it a valuable tool for altering a material's structure and thus improving our understanding of correlations between nanostructure and magnetism.

This paper compares the magnetic behavior of two mechanically milled alloys. $SmCo_5$ and $GdAl_2$ are both ferromagnetic in their crystalline state. The goal of this paper is to understand how the nanostructure produced by mechanical milling affects the ferromagnetism and, in particular, how milling can induce a change in magnetic ordering from ferromagnetic to spin-glass-like. The first section of this paper details sample fabrication and the characterization techniques used to determine the nanostructure of the samples. Magnetic measurements are described in the second section of the paper and followed by a discussion of the correlations between nanostructure and magnetic properties.

EXPERIMENTAL DETAILS

Sample fabrication

Commercially purchased $SmCo_5$ powder (-100 mesh) was handled exclusively in an argon-filled glove box to prevent oxidation. Milling was performed in a hermetically sealed tungsten-carbide-lined vial in a SPEX 8000 mixer/mill with a 3:1 ball-to-powder mass ratio. The three milling balls were also made of tungsten carbide. Milling was stopped every 15 minutes for the first two hours and every hour thereafter to remove a small amount of powder for x-ray diffraction and magnetic measurements, and to break up powder clumps. Milling continued for a total of 30 hours in fifteen-minute intervals. Fifteen-minute rest periods between milling segments were used to minimize heating.

The starting $GdAl_2$ bulk sample was formed by arc melting Gd (99.9%) and Al (99.999%) shot in an argon atmosphere. The bulk sample was ground to a powder, then annealed at 800°C for 48 hours in a vacuum of $\sim 10^{-6}$ torr. Milling was performed in a tungsten-carbide-lined vial in a SPEX 8000 mixer/mill for times up to 400 hours. A one-to-one ball-to-powder mass ratio was used with one tungsten-carbide ball. As with the $SmCo_5$, all milling and handling was performed in an argon atmosphere to minimize contamination and the sample was milled in fifteen-minute increments with fifteen-minute breaks to minimize heating.

Structural and magnetic measurements

X-ray diffraction patterns were obtained using a D-Max-B Rigaku diffractometer with Cu-K_α radiation. Bright-field transmission electron micrographs were taken using a 200 kV JEOL 2010 high-resolution microscope. Sample preparation for the $SmCo_5$ consisted of encapsulating milled powder in a room-temperature-cured epoxy and microtoming with a diamond knife to a thickness of approximately 100 nm. $GdAl_2$ powders were ultrasonicated in isopropanol and deposited on a carbon-coated Cu TEM grid.

Samples for magnetic measurements were loaded in paraffin-filled polyethylene bags in the glove box and sealed. The paraffin was melted to immobilize the randomly oriented powder particles during measurement. The polyethylene bags also protected the samples from oxidation during the transfer from the glovebox to the magnetometers. The coercivity (H_c) and remanence ratio (M_r/M_s, where M_r is the remanence ratio and M_s is the saturation magnetization) of the $SmCo_5$ were extracted from room temperature hysteresis loops.

Temperature-dependent magnetization measurements of $SmCo_5$ and $GdAl_2$ were made at fields from 100 Oe to 500 Oe using a Quantum Design MPMS SQUID magnetometer. The zero-

field-cooled (ZFC) magnetization was measured by cooling the sample to 5 K with no applied field, stabilizing the temperature, then applying the field and measuring as the temperature was increased to 300 K. The field-cooled (FC) magnetization was measured by apply the measuring field at 300 K and taking data as the sample was cooled.

Low-field magnetization measurements of $GdAl_2$ from 1 Oe to 100 Oe were made using a Quantum Design MPMS XL7 SQUID magnetometer with a magnet-reset option. The same procedure was used to measure the ZFC and FC magnetizations at low field, except that the sample was held at or above 250 K and the magnet quenched to reduce the residual field to < 0.5 Oe before cooling to 5 K and making FC and ZFC measurements as described above.

DISCUSSION

Evolution of the nanostructure

Figures 1a and 1b show the changes in the x-ray diffraction patterns with milling time for $SmCo_5$ and $GdAl_2$. The initial material in both cases has fairly sharp x-ray diffraction peaks at the same Bragg angles as those expected for the bulk materials. The annealing of the $GdAl_2$ prior to milling produces a much larger starting grain size and the diffraction peaks are correspondingly sharper. As milling time increases, the diffraction peaks of both materials become increasingly broad and diffuse, indicating grain refinement and disordering of the alloy.

The (110) $SmCo_5$ diffraction peak was Fourier decomposed and compared to a LaB_6 standard to remove instrumental broadening and contributions from the $K_{\alpha 2}$ doublet [4]. A single-profile analysis that separates linewidth broadening due to microstrain from broadening due to grain size was applied to extract the coherent diffracting crystallite size (DCS) and root-mean-squared microstrain [5]. The $GdAl_2$ data were analyzed using an integral-breadth technique after the $K_{\alpha 2}$ contributions were removed from the (111) diffraction peak.

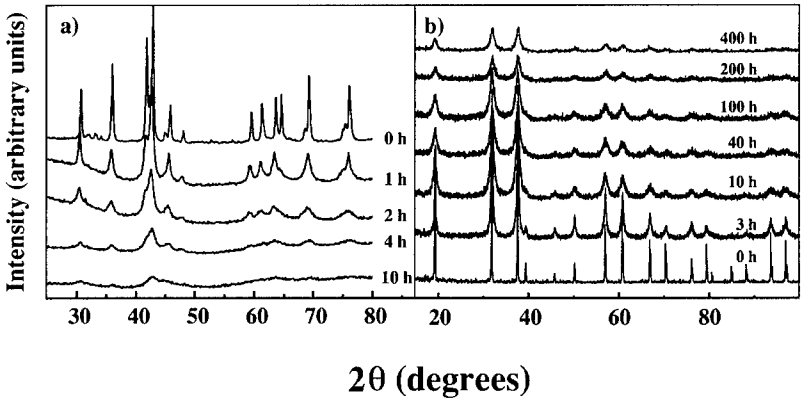

Figure 1. X-ray diffraction patterns for a) $SmCo_5$ and b) $GdAl_2$ as functions of milling time.

Figure 2 shows the DCSs as functions of milling time for the $SmCo_5$ and $GdAl_2$. The $SmCo_5$ grain size rapidly decreases from 20 nm to ~5 nm after only 4 hours of milling [6]. The $GdAl_2$ also experiences rapid reduction from its initial grain size of 90 nm, but takes considerably longer time to reach its final mean grain size of ~8 nm. The minimum attainable grain size depends on the melting temperature of the material; however, milling intensity and temperature also play important roles in determining the final grain size [7]. The structures presented are the results for two specific sets of processing parameters. Fabrication parameters can be varied to produce other nanostructures.

Transmission electron microscopy (TEM) was performed to further investigate the effects of milling on the morphology. TEM shows that the milled powder particles are close to spherical in shape, with a distribution of particle sizes. Figure 3 shows particle-size distributions from $GdAl_2$ milled for 300 hours and 400 hours. The mean grain size obtained from x-ray diffraction measurements remains constant over this range of milling times, and agrees well with the mean grain size obtained from the TEM measurements. Note that the sample preparation technique for the TEM grain-size-distribution measurement eliminates very large particles, so the possibility of there being larger single-or multi-grain particles remains.

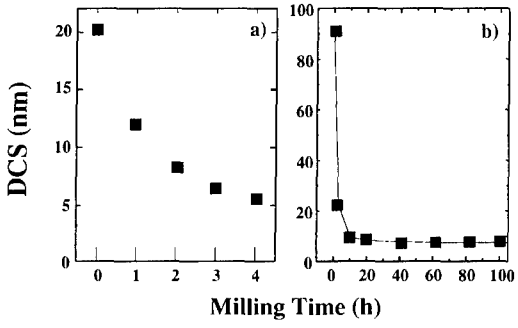

Figure 2: The dependence of coherent diffracting crystallite size (DCS) on milling time for a) $SmCo_5$ and b) $GdAl_2$.

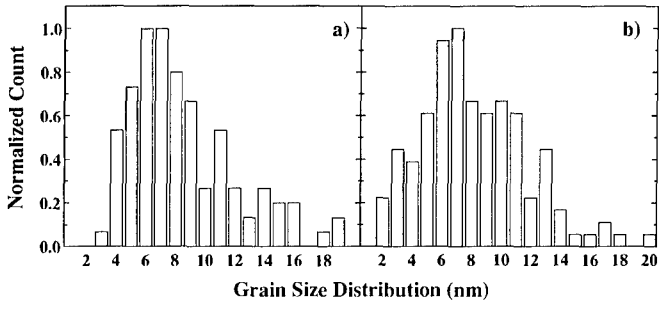

Figure 3: Particle size distribution for $GdAl_2$ milled for a) 300 hours and b) 400 hours. The mean grain size obtained from x-ray diffraction measurements is 8 nm for both samples.

Magnetic properties

Milling time is in general not a robust parameter for characterizing nanostructure due to the complex dependence of nanostructure on milling intensity, temperature, and other factors; however, $SmCo_5$ grains are refined to the limits within which a grain size can be obtained from x-ray diffraction within the first four hours of milling. We therefore must settle for parameterizing these data in terms of milling time.

Figure 4 shows the dependence of the coercivity H_c and the remanence ratio M_r/M_s on milling time for $SmCo_5$. The dependence of the coercivity on milling time appears similar to that expected for particles passing from multi-domain to single domain and finally to superparamagnetic sizes; however, the grain size changes from 20 nm to 4 nm during the period of greatest change in the magnetic properties.

Aging studies were used to probe the origin of the enhanced coercivity. The coercivity of $SmCo_5$ milled for 2 hours decreases by a factor of two over the two-week period immediately following the milling [8]. Measurements of the same samples were made every 48 hours for two weeks, with the samples stored in an Ar-filled glove box at room temperature in between measurements. The coercivity was constant after two weeks of aging. No changes in grain size were observed using x-ray diffraction; however, the diffraction peak positions shifted slightly toward higher angles as the samples aged. The large coercivity change at constant grain size eliminates grain size effects as the source of the enhanced coercivity. The shift in diffraction peak positions suggests that defects and strain play a large role in the magnetic properties. We attribute the increase in coercivity to the milling-induced defects and/or strain, which are metastable enough to be removed by room temperature annealing. The saturation magnetization decreased by only 0.1% during this time, so the coercivity decrease is not attributable to oxidation.

Figure 4 shows that the coercivity increases only during the first two hours of milling. Samples milled for longer times show lower coercivities and remanence ratios, although the remanence ratio remains above 0.5 for all milling times.

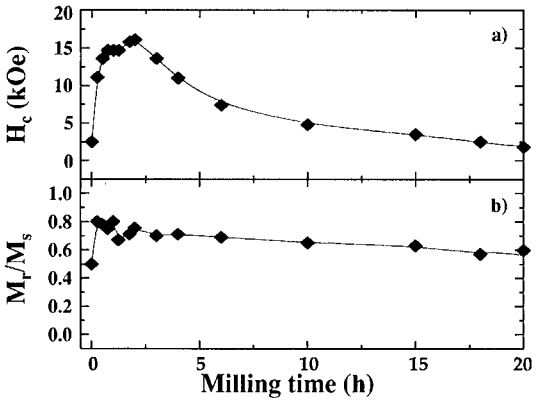

Figure 4. The dependence of a) the coercivity (H_c) and b) the remanence ratio (M_r/M_s) on milling time for $SmCo_5$.

Irreversibility between the field-cooled (FC) and zero-field-cooled (ZFC) low-field magnetizations increases as milling time increases. Figure 5 shows the magnetization at 100 Oe for $SmCo_5$ milled for 4 hours (top) and 15 hours (bottom). FC and ZFC magnetizations obey a $T^{3/2}$ behavior after 4 hours of milling; however, the sample milled for 15 hours shows a departure from the $T^{3/2}$ behavior at lower temperatures, and irreversibility between the FC and ZFC magnetizations. Subtracting the $T^{3/2}$ behavior shows that the remaining magnetization has a broad peak at low temperatures. Small cobalt clusters form for milling times greater than 20 hours, which prevents further investigation of the magnetically glassy phase.

Monitoring a paramagnet/ferromagnet or paramagnet/magnetic-glass transition in a high-Curie-temperature material such as $SmCo_5$ (T_c ~1000 K) is difficult because measurement at high temperatures would significantly change the nanostructure. $GdAl_2$ is a ferromagnet in its crystalline phase and shows spin-glass-like behavior when amorphous. The lower Curie temperature (T_c ~ 175 K) allows investigation of the paramagnet/ferromagnet transition without any temperature-induced nanostructure changes.

Earlier measurements of mechanically milled $GdAl_2$ showed irreversibility between the FC and ZFC magnetizations, and a broad peak spin-glass-like peak; however, the peak temperature occurs near 60 K instead of the 16 K freezing temperature found in amorphous $GdAl_2$ films [9,10]. Figure 6 shows the $GdAl_2$ zero-field-cooled magnetization at 100 Oe for milling times up to 80 hours. Unmilled $GdAl_2$ shows the characteristic ferromagnetic behavior. The transition lessens in magnitude and a broad peak near 45 K appears after 3 hours of milling. The peak continues to broaden and shifts to ~ 50 K after 80 hours of milling.

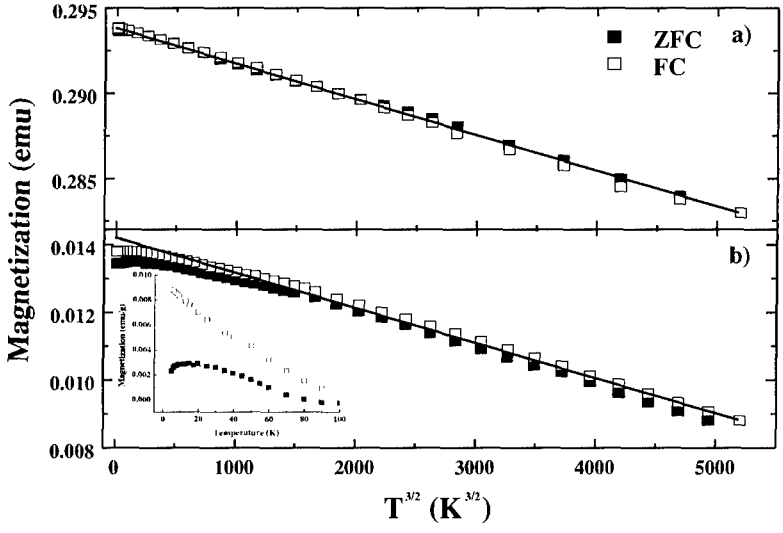

Figure 5. The field-cooled (FC) and zero-field-cooled (ZFC) magnetizations measured at 100 Oe for $SmCo_5$ milled for a) 4 hours and b) 15 hours. The FC magnetization is represented by open symbols and the ZFC magnetization is represented by solid symbols. The inset shows the FC and ZFC magnetizations for the 15-hour milled sample with the $T^{3/2}$ behavior removed.

Figure 2b shows that the $GdAl_2$ reaches its final grain size of 8 nm after 40 hours of milling; however, the magnetic properties continue to change with additional milling, despite the lack of further grain reduction. This indicates that disordering is the dominant effect of extended milling. Although the data in Figure 6 appear to show that ferromagnetism has disappeared by 80 hours of milling, measurements at lower fields reveal residual ferromagnetism. Figure 7 shows the FC and ZFC magnetizations in a field of 5 Oe for samples milled for 200 h and 300 h. The position of the peak measured in a field of 5 Oe occurs at the same temperature as the measurements at 100 Oe, in contrast to earlier reports [9,10]. As in the case of $SmCo_5$, ferromagnetic and spin-glass-like behaviors are observed, although the ferromagnetic component in $GdAl_2$ is weaker. The magnitude of the magnetization for the 300 h data is larger than for the 200 h data, which suggests that the proportion of the sample in the spin-glass-like phase

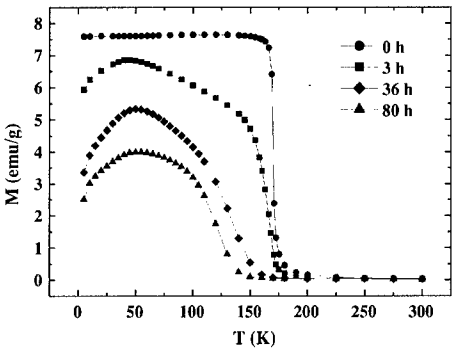

Figure 6. The dependence of the magnetization on the milling time for $GdAl_2$. All data were taken in a field of 100 Oe in the ZFC configuration.

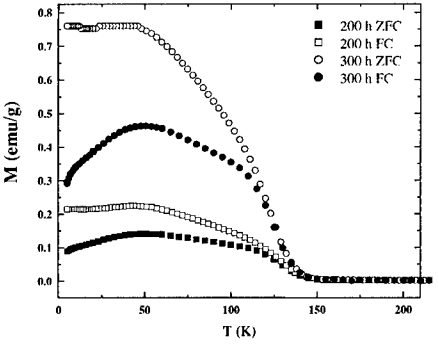

Figure 7. The dependence of the magnetization at 5 Oe on the milling time for $GdAl_2$ milled for 200 h (squares) and 300 h (circles). The ZFC data are represented by solid symbols and the FC data by open symbols.

increases with milling time. The observed behavior differs from canonical spin-glass behavior in that the separation between the FC and ZFC curves occurs at a much higher temperature than the peak temperature, and that the FC magnetization displays a large offset relative to the ZFC magnetization. Lower-field measurements indicate that the separation point between the FC and ZFC curves shown near 120 K in Figure 7 is actually coincident with a second magnetic transition. The ZFC magnetization at 1 Oe for 300-hour milled $GdAl_2$ (Figure 8) shows the presence of the second magnetic transition more clearly.

The relationship between nanostructure and magnetism

The magnetic properties of our mechanically milled $GdAl_2$ are different than those observed by Zhou and Bakker (ZB) [9,10]; however, the physical origins of the magnetically glassy behavior can be elucidated by investigating how differences in nanostructure affect magnetic properties. Mechanical milling of $GdAl_2$ has two primary effects: the introduction of quadruple-defect disorder and grain refinement. Quadruple-defect disorder results from the large difference between the sizes of Gd and Al atoms, which allows Al to substitute on the Gd sublattice, but prevents Gd from substituting on the Al lattice. ZB used low-intensity milling and started with a grain size of about 45 nm, while our experiment used high-intensity milling and a larger starting grain size of about 90 nm. The milling intensity and degree of disorder of the starting materials can significantly affect the nanostructure of the final material and thus its magnetic properties. The volume ratio of crystalline to amorphous phases, and the degree of disorder within and at the surface of the grains also play important roles in determining magnetic properties. Our results underscore the sensitivity of magnetic properties to nanostructure.

The initial stages of milling produce an exponential decrease in the crystallite size, along with the introduction of small amounts of disorder. The decrease of the Curie temperature with milling time could indicate finite size effects on the Curie temperature due to grain refinement, and/or the effect of disorder weakening the Gd-Gd exchange. Once the grain size has reached its minimum value, the dominant effect of continued milling is to increase disorder. This is consistent with changes in the magnetic properties that are observed after the mean grain size has reached a steady state.

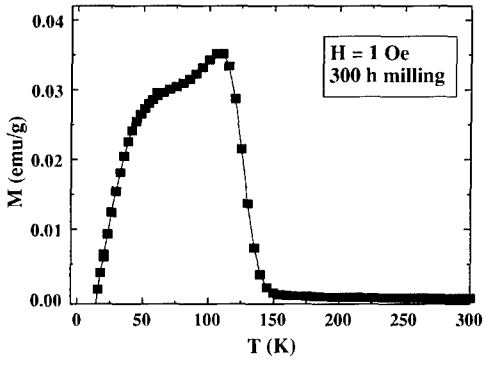

Figure 8. The magnetization of $GdAl_2$ after 300 hours of milling in a measuring field of 1 Oe.

ZB's $GdAl_2$ 'spin-glass' sample has a mean grain size of 20 nm. The majority of the atoms are in the bulk, which suggests that the broad peak in the ZFC magnetization is characteristic of grains of disordered $GdAl_2$. Finite-size effects are not expected to be significant at a grain size of 21 nm. ZB observe a feature in the ZFC magnetization near 16 K – the temperature at which amorphous $GdAl_2$ shows a freezing transition. Although ZB do not address this feature specifically, it is likely that some significantly amorphized material is present.

Although our nanostructured $GdAl_2$, with a final mean grain size of 8 nm, has a much larger fraction of atoms on surfaces or interfaces, ferromagnetic interactions remain dominant enough to produce a strong ferromagnetic transition, albeit with a lower Curie temperature than the bulk. Additional investigation of the effect of milling parameters on the final nanostructure is underway so as to produce a sample free of ferromagnetic effects.

Modder and Bakker found a combination of magnetically glassy and ferromagnetic behavior in mechanically milled $GdIr_2$ with a grain size of ~10 nm [11]. Gd and Ir are much closer in atomic diameter than Gd and Al, Gd can be transferred to the Ir sublattice and vice-versa. Ferromagnetic and spin-glass-like transitions (at 150 K and 20 K) are observed in mechanically milled $GdIr_2$. Modder and Bakker call this a re-entrant spin glass; however, it is more likely that their nanostructured $GdIr_2$ is a two-phase system, with one phase responsible for the ferromagnetic behavior and one responsible for the spin-glass-like behavior. The role of the non-magnetic element in mediating Gd-Gd coupling was cited by Modder and Bakker as important in explaining the differences in the magnetic properties of $GdIr_2$ and $GdAl_2$. Our results show that it is possible to obtain two-phase behavior similar to that found in $GdIr_2$ in $GdAl_2$ with the appropriate nanostructure.

The degree of long-range order appears to be critical to the observation and temperature of the peak in the ZFC magnetization. Magnetic and structural measurements of $GdAl_2$ thin films indicate the presence of ferromagnetic order on a length scale of 2-4 nm [12]. The observed 16 K freezing temperature of $GdAl_2$ films may be due to coupled ferromagnetic regions with random orientation. Rettori, et al. found that Gd can induce significant random anisotropy effects [13]. Amorphous Gd_xAl_{1-x} is spin-glass-like for $x \leq 0.4$ and ferromagnetic for $0.56 < x < 0.81$. A peak in the susceptibility for $0.4 < x < 0.56$ is observed in low-field measurements; however, the same samples showed ferromagnetic behavior in high-field measurements [14]. The observation of different behaviors in the same sample can be clarified by Figures 7 and 8. The components in the two-phase system respond differently to the magnetic field. The relative amounts of each phase, the measuring field and the temperature determine whether ferromagnetic or spin-glass-like responses dominate the magnetization. Mechanically alloyed $Ag_{95}Gd_5$ has a spin-glass-like peak was observed near 5K that is attributed to interacting ferromagnetic Gd clusters with diameters on the order of a few nanometers [15]. These observations suggest that sample homogeneity and its effect on short-range magnetic order is critical to understanding the nature of magnetic ordering in glassy materials.

CONCLUSIONS

The properties of nanostructured ferromagnetic alloys change significantly with grain size and the amount of disorder introduced during mechanical milling. This sensitive dependence may be taken advantage of to explore the relative importance of grain size and disorder in determining magnetic properties. $SmCo_5$ exhibits enhanced coercivities and large remanence ratios when milled for short periods of time. The coercivity increase is attributed to the

formation of defects and increased strain, which can be removed by room temperature annealing. Continued milling produces irreversibility between field-cooled and zero-field cooled magnetizations at low fields, along with the appearance of a broad peak at low temperatures. Cobalt clustering results from extended milling, effectively limiting investigation of the phase responsible for the magnetically glassy behavior.

$GdAl_2$ has a lower Curie temperature (175 K) and undergoes a spin-glass-like transition in the amorphous phase, making it an ideal system in which to study the origins of magnetically glassy behavior. High-intensity milling was used to produce nanostructured $GdAl_2$ with a mean grain size of 8 nm. Magnetic measurements showed the presence of a ferromagnetic transition at 120 K and a broad peak at 50 K. The effect of disorder and intergrain interactions must be investigated to determine whether the broad peaks observed in nanostructured ferromagnets are truly indicative of spin-glass-like transitions.

ACKNOWLEDGEMENTS

The authors would like to thank D.J. Sellmyer, R.D. Kirby and R. Skomski for their advice and discussions. Research was supported by the Air Force Office of Scientific Research, the UNL Center for Materials Research and Analysis, and the National Science Foundation through grants DMR-98-75425, DMR-99-72196 and DMR-99-75887.

REFERENCES

1) C.C. Koch, NanoStruct. Mater. **2**, 109 (1993).
2) C. Suryanrayana, Prog. Mater. Sci. **46**, 1 (2001).
3) C.C. Koch, Scripta Met. **34**, 21 (1996).
4) A.R. Stokes, Proc. Phys. Soc. London **61**, 382 (1948).
5) P. Ganesan, H.K. Kuo, A. Saavedra, and R.J. DeAngelis, J. Catal. **52**, 310 (1978).
6) Diandra L. Leslie-Pelecky and Richard L. Schalek, Phys. Rev. B **59**, 457 (1999).
7) J. Eckert, J.C. Holzer, C.E. Krill III, and W.L. Johnson, J. Mater. Res. **7**, 1751 (1992).
8) Diandra L. Leslie-Pelecky, E.M. Kirkpatrick, and R.L. Schalek, Nanostruct. Mater. **12**, 887 (1999).
9) G.F. Zhou and H. Bakker, Phys. Rev. Lett. **73**, 344 (1994).
10) G.F. Zhou and H. Bakker, Phys. Rev. B **52**, 9437 (1995).
11) I.W. Modder and H. Bakker, Phys. Rev. B **58**, 14479 (1998).
12) S.C. Hart, P.E. Wigen, and A.P. Malozemoff, J. Appl. Phys. **50**, 1620 (1979).
13) C. Rettori, D. Davidov, R. Orbach, and E.P. Chock, Phys. Rev. B **7**, 1 (1973).
14) T.R. McGuire, T. Mizoguchi, R.J. Gambino, and S. Kirkpatrick, J. Appl. Phys **49** (1978).
15) J. Tang, W. Zhao, J. O'Connor, C. Tao, and L. Wang, Phys. Rev. B **52**, 12829 (1995).